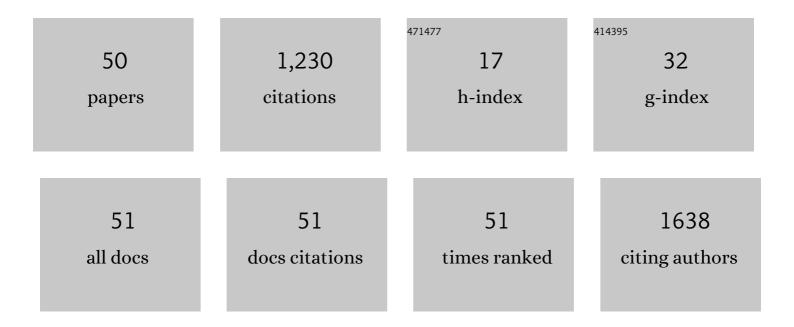
Jian-hua Zhou

List of Publications by Year in descending order

Source: https://exaly.com/author-pdf/8184816/publications.pdf Version: 2024-02-01



#	Article	IF	CITATIONS
1	Multiparametric Quantitative US Examination of Liver Fibrosis: A Feature-Engineering and Machine-Learning Based Analysis. IEEE Journal of Biomedical and Health Informatics, 2022, 26, 715-726.	6.3	6
2	The uncertainty of boundary can improve the classification accuracy of Blâ€RADS 4A ultrasound image. Medical Physics, 2022, 49, 3314-3324.	3.0	1
3	Contrast-Enhanced Ultrasound Using Perfluorobutane: Impact of Proposed Modified LI-RADS Criteria on Hepatocellular Carcinoma Detection. American Journal of Roentgenology, 2022, 219, 434-443.	2.2	10
4	Comparison of diagnostic accuracy and utility of artificial intelligence–optimized ACR TI-RADS and original ACR TI-RADS: a multi-center validation study based on 2061 thyroid nodules. European Radiology, 2022, 32, 7733-7742.	4.5	12
5	Elaboration and Validation of a Nomogram Based on Axillary Ultrasound and Tumor Clinicopathological Features to Predict Axillary Lymph Node Metastasis in Patients With Breast Cancer. Frontiers in Oncology, 2022, 12, .	2.8	7
6	Radiofrequency ablation of benign thyroid nodules: Recommendations from the Asian conference on tumor ablation task force – Secondary publication. Journal of Medical Ultrasound, 2021, 29, 77.	0.4	10
7	Clinical Application of Liver Imaging Reporting and Data System for Characterizing Liver Neoplasms: A Meta-Analysis. Diagnostics, 2021, 11, 323.	2.6	12
8	Diagnosis of Non-Hepatocellular Carcinoma Malignancies in Patients With Risks for Hepatocellular Carcinoma: CEUS LI-RADS Versus CT/MRI LI-RADS. Frontiers in Oncology, 2021, 11, 641195.	2.8	7
9	Validation of American College of Radiology Ovarian-Adnexal Reporting and Data System Ultrasound (O-RADS US): Analysis on 1054 adnexal masses. Gynecologic Oncology, 2021, 162, 107-112.	1.4	52
10	Value of dual-phase, contrast-enhanced CT combined with ultrasound for the diagnosis of metastasis to central lymph nodes in patients with papillary thyroid cancer. Clinical Imaging, 2021, 75, 5-11.	1.5	7
11	Quantitative analysis of shear wave elastic heterogeneity for prediction of lymphovascular invasion in breast cancer. British Journal of Radiology, 2021, 94, 20210682.	2.2	6
12	Radiofrequency ablation of benign thyroid nodules: recommendations from the Asian Conference on Tumor Ablation Task Force. Ultrasonography, 2021, 40, 75-82.	2.3	37
13	Distinguishing intrahepatic cholangiocarcinoma from hepatocellular carcinoma in patients with and without risks: the evaluation of the LR-M criteria of contrast-enhanced ultrasound liver imaging reporting and data system version 2017. European Radiology, 2020, 30, 461-470.	4.5	44
14	Added Value of Different Types of Elastography in Evaluating Ultrasonography Detected Breast Lesions: A Compared Study With Mammography. Clinical Breast Cancer, 2020, 20, e366-e372.	2.4	7
15	Evaluation of Contrast-enhanced US LI-RADS version 2017: Application on 2020 Liver Nodules in Patients with Hepatitis B Infection. Radiology, 2020, 294, 299-307.	7.3	73
16	Core Needle Biopsy Targeting the Viable Area of Deep-Sited Dominant Lesion Verified by Color Doppler and/or Contrast-Enhanced Ultrasound Contribute to the Actionable Diagnosis of the Patients Suspicious of Lymphoma. Frontiers in Oncology, 2020, 10, 500153.	2.8	3
17	Evaluation of the Extent of Mesorectal Invasion and Mesorectal Fascia Involvement in Patients with T3 Rectal Cancer With 2-D and 3-D Transrectal Ultrasound: A Pilot Comparison Study With Magnetic Resonance Imaging Findings. Ultrasound in Medicine and Biology, 2020, 46, 3008-3016.	1.5	1
18	Deep learning radiomics can predict axillary lymph node status in early-stage breast cancer. Nature Communications, 2020, 11, 1236.	12.8	276

JIAN-HUA ZHOU

#	Article	IF	CITATIONS
19	Spatial Characterization of Tumor Perfusion Properties from 3D DCE-US Perfusion Maps are Early Predictors of Cancer Treatment Response. Scientific Reports, 2020, 10, 6996.	3.3	9
20	Shear-Wave Elastography of the Breast: Added Value of a Quality Map in Diagnosis and Prediction of the Biological Characteristics of Breast Cancer. Korean Journal of Radiology, 2020, 21, 172.	3.4	19
21	Reducing Unnecessary Biopsy of Breast Lesions: Preliminary Results with Combination of Strain and Shear-Wave Elastography. Ultrasound in Medicine and Biology, 2019, 45, 2317-2327.	1.5	19
22	Early differentiating between the chemotherapy responders and nonresponders: preliminary results with ultrasonic spectrum analysis of the RF time series in preclinical breast cancer models. Cancer Imaging, 2019, 19, 61.	2.8	4
23	Shear Wave Elastography of Breast Lesions: Quantitative Analysis of Elastic Heterogeneity Improves Diagnostic Performance. Ultrasound in Medicine and Biology, 2019, 45, 1909-1917.	1.5	10
24	Pharmacokinetic Modeling of Targeted Ultrasound Contrast Agents for Quantitative Assessment of Anti-Angiogenic Therapy: a Longitudinal Case-Control Study in Colon Cancer. Molecular Imaging and Biology, 2019, 21, 633-643.	2.6	9
25	Combination of different types of elastography in downgrading ultrasound Breast Imaging-Reporting and Data System category 4a breast lesions. Breast Cancer Research and Treatment, 2019, 174, 423-432.	2.5	19
26	Identification of a 4â€ <scp>mRNA</scp> metastasisâ€related prognostic signature for patients with breast cancer. Journal of Cellular and Molecular Medicine, 2019, 23, 1439-1447.	3.6	25
27	Association Between Shear Wave Elastography of Virtual Touch Tissue Imaging Quantification Parameters and the Kiâ€67 Proliferation Status in Luminalâ€Type Breast Cancer. Journal of Ultrasound in Medicine, 2019, 38, 73-80.	1.7	7
28	Diagnostic value, safety, and histopathologic discrepancy risk factors for endoscopic forceps biopsy and transrectal ultrasound-guided core needle biopsy in rectum lesions. Annals of Translational Medicine, 2019, 7, 607-607.	1.7	4
29	Anatomical Road Mapping Using CT and MR Enterography for Ultrasound Molecular Imaging of Small Bowel Inflammation in Swine. European Radiology, 2018, 28, 2068-2076.	4.5	1
30	Efficacy of ultrasound-guided core needle biopsy in cervical lymphadenopathy: A retrospective study of 6,695 cases. European Radiology, 2018, 28, 1809-1817.	4.5	45
31	Contrast-Enhanced Ultrasound Improves the Pathological Outcomes of US-Guided Core Needle Biopsy That Targets the Viable Area of Anterior Mediastinal Masses. BioMed Research International, 2018, 2018, 1-9.	1.9	13
32	Ultrasonic RF time series for early assessment of the tumor response to chemotherapy. Oncotarget, 2018, 9, 2668-2677.	1.8	6
33	Early prediction of tumor response to bevacizumab treatment in murine colon cancer models using three-dimensional dynamic contrast-enhanced ultrasound imaging. Angiogenesis, 2017, 20, 547-555.	7.2	26
34	Combined Hepatocellular Cholangiocarcinoma (Biphenotypic) Tumors: Potential Role of Contrast-Enhanced Ultrasound in Diagnosis. American Journal of Roentgenology, 2017, 209, 767-774.	2.2	9
35	Early Detection and Assessment of Liver Fibrosis by using Ultrasound RF Time Series. Journal of Medical and Biological Engineering, 2017, 37, 717-729.	1.8	10
36	The prognostic value of the preoperative c-reactive protein/albumin ratio in ovarian cancer. BMC Cancer, 2017, 17, 285.	2.6	98

Jian-hua Zhou

#	Article	IF	CITATIONS
37	Morphine, a potential antagonist of cisplatin cytotoxicity, inhibits cisplatin-induced apoptosis and suppression of tumor growth in nasopharyngeal carcinoma xenografts. Scientific Reports, 2016, 6, 18706.	3.3	42
38	VEGFR2-Targeted Three-Dimensional Ultrasound Imaging Can Predict Responses to Antiangiogenic Therapy in Preclinical Models of Colon Cancer. Cancer Research, 2016, 76, 4081-4089.	0.9	38
39	Comparative Proteomics Reveals Important Viral-Host Interactions in HCV-Infected Human Liver Cells. PLoS ONE, 2016, 11, e0147991.	2.5	2
40	Quantitative Contrast-Enhanced Ultrasonic Imaging Reflects Microvascularization in Hepatocellular Carcinoma and Prognosis after Resection. Ultrasound in Medicine and Biology, 2015, 41, 2621-2630.	1.5	7
41	Dose-response relationship in cisplatin-treated breast cancer xenografts monitored with dynamic contrast-enhanced ultrasound. BMC Cancer, 2015, 15, 136.	2.6	16
42	A Novel Class of Small Molecule Compounds that Inhibit Hepatitis C Virus Infection by Targeting the Prohibitin-CRaf Pathway. EBioMedicine, 2015, 2, 1600-1606.	6.1	49
43	The Degree of Contrast Washout on Contrast-Enhanced Ultrasound in Distinguishing Intrahepatic Cholangiocarcinoma from Hepatocellular Carcinoma. Ultrasound in Medicine and Biology, 2015, 41, 3088-3095.	1.5	42
44	Ultrasonic spectrum analysis for in vivo characterization of tumor microstructural changes in the evaluation of tumor response to chemotherapy using diagnostic ultrasound. BMC Cancer, 2013, 13, 302.	2.6	7
45	Quantitative Assessment of Tumor Blood Flow Changes in a Murine Breast Cancer Model After Adriamycin Chemotherapy Using Contrast-Enhanced Destruction-Replenishment Sonography. Journal of Ultrasound in Medicine, 2013, 32, 683-690.	1.7	10
46	Assessment of Early Tumor Response to Cytotoxic Chemotherapy with Dynamic Contrast-Enhanced Ultrasound in Human Breast Cancer Xenografts. PLoS ONE, 2013, 8, e58274.	2.5	26
47	Contrast-enhanced ultrasonic parametric perfusion imaging in the evaluation of antiangiogenic tumor treatment. European Journal of Radiology, 2012, 81, 1360-1365.	2.6	18
48	Quantitative Assessment of Tumor Blood Flow in Mice after Treatment with Different Doses of an Antiangiogenic Agent with Contrast-enhanced Destruction-Replenishment US. Radiology, 2011, 259, 406-413.	7.3	31
49	Contrast-Enhanced Gray-Scale Ultrasound for Quantitative Evaluation of Tumor Response to Chemotherapy: Preliminary Results With a Mouse Hepatoma Model. American Journal of Roentgenology, 2011, 196, W13-W17.	2.2	19
50	Antiangiogenic Tumor Treatment. Academic Radiology, 2010, 17, 646-651.	2.5	9